

Development of Low-Exergy-Loss, High-Efficiency Chemical Engines

Investigators

Christopher F. Edwards, Associate Professor, Mechanical Engineering; Kwee-Yan Teh
Shannon L. Miller, Matthew N. Svrcek, Graduate Researchers, Stanford University.

Abstract

Recent progress in our effort to develop ultra-high efficiency, low-exergy loss engines is reported. The work is divided into two tasks. In the first an experimental system capable of engaging the critical issues associated with extreme-state combustion is being developed. In the second we continue our work to define in a rigorous way the approach required to developing low-exergy loss engines.

For the first task, progress centers around definition and construction of the prototype system. The key high-pressure components have been designed and fabricated and are currently awaiting assembly. Poppet valve testing has been conducted and used to define the gas transfer requirements for achieving rapid, high compression. Ring analyses have been conducted and suitable approaches for dealing with high-speed, high-pressure sealing have been identified.

For the second task, progress centers around extension of the dynamical system model to include active and passive transfers of heat and matter. This extension places these energy interactions on an even footing with energy transfer as work in the analysis previously conducted for closed, adiabatic systems. This work completes the analysis of combustion engines at the simple cycle level and lays the groundwork for our next stage of efforts that incorporate regeneration into the analysis framework.

Introduction

An engine is a device that converts some fraction of the energy in a resource into work. The most work that can be developed by a particular engine design is its reversible work. The irreversibility of an engine is the difference between the reversible work that it could develop and the actual work that it performs; it is the lost work.

In this project, we investigate the potential to design and implement chemical engines with significantly reduced irreversibility, and thereby, improved efficiency. The relevance of this work to the objective of GCEP is that significant improvements in efficiency are one of the most effective approaches to reducing greenhouse-gas emissions.

In the case of simple-cycle combustion engines, state-of-the-art engine first-law efficiencies (work per unit LHV) are less than 50%, due to exergy destruction during combustion, heat transfer losses, and poor extraction (high exhaust enthalpy). We have previously shown that a rapid, extreme compression/expansion approach is necessary to substantially reduce these losses so as to achieve engine efficiencies well beyond 50%.

This project includes two parts: an experimental component to construct a device to demonstrate the feasibility and efficiency potential of combustion at such extreme

conditions, and a theoretical component, to continue our investigations into the possible pathways to realizing ultra-high-efficiency engines.

Background

In our previous work we showed that the only way to reduce exergy destruction during combustion is to move the reactants to higher internal energy states prior to reaction. While there are a number of ways to accomplish this, raising the compression ratio (using work to increase the reactant internal energy), is the best matched to the expansion process used to extract work from the product gases. A second option, heat transfer into the system, also transfers in entropy, pushing the system farther away from the optimal expansion path. The details of these conclusions are described in last year's GCEP Technical Report [1].

Figure 1 shows the theoretical first-law efficiency for adiabatic Otto (symmetric compression/expansion) and Atkinson (ideally expansion) cycles. The colored bands show 70-80% of these efficiencies, representing a range for typical efficiencies achieved when implemented in real engines. At compression ratios of 100:1 and higher, the 70-80% bands surpass 50%. One of the main goals for this project is to demonstrate the feasibility of reduced irreversibility using extreme compression.

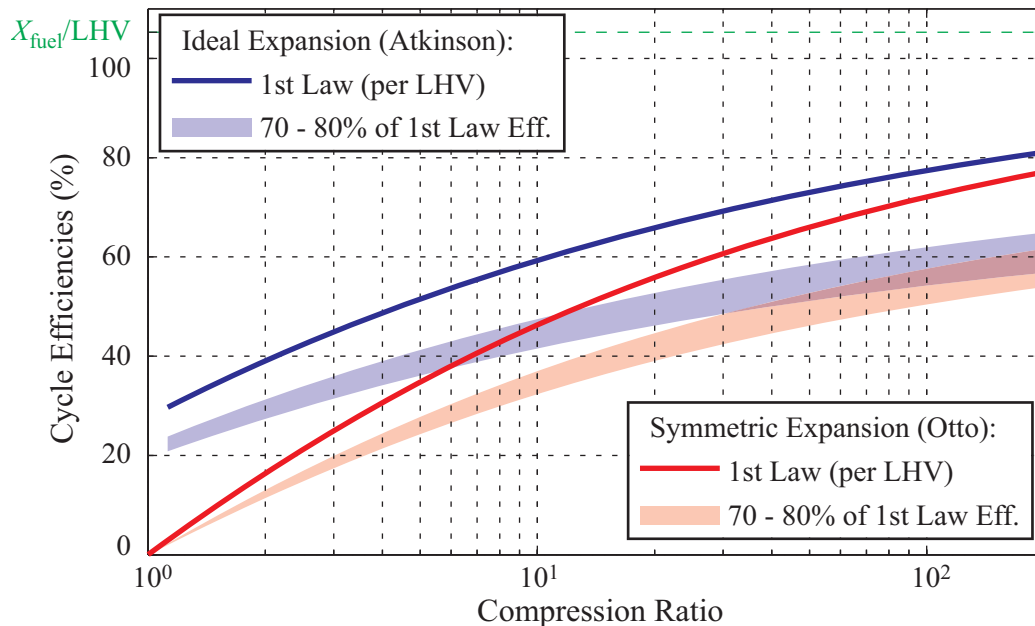


Figure 1: Otto and Atkinson cycle efficiencies for stoichiometric propane/air. The red and blue bands represent 70-80% of the first law efficiencies, which is what current engines often achieve in practice after implementation efficiencies are included.

In the experimental part of this program, our work has been focused on developing the hardware necessary to implement the extreme compression process on a single-shot, laboratory demonstration basis. In the theoretical part, the previous work has been extended to include the possibilities of arbitrary, active matter and heat transfer interactions with the working fluid in the cylinder. Passive losses, including both heat and mass loss (blowby) have also been included. A summary of the results and progress on these two topics is given below.

Progress and Results

Task 1: Demonstration of Low-Irreversibility Combustion by Extreme Compression

The majority of this past year has been spent refining the experimental design for the extreme compression/expansion device and building the required hardware. To demonstrate feasibility of performing combustion at extreme states, we are building a single-shot, high-compression device. The device is designed to achieve volumetric compression ratios of greater than 100:1 and will utilize a direct-injection, PCCI-like combustion strategy to achieve reaction phasing. Our objective is to measure the indicated work achievable using this strategy, and thereby the potential engine efficiency. While our objective is to demonstrate the viability and efficiency of the proposed extreme-compression combustion strategy, we note that researchers at other laboratories (e.g., Sandia National Labs [2]) are currently investigating the issues associated with development of linear-alternator free-piston engines. This type of engine would be well suited to practical implementation of our extreme-compression concept.

A diagram of the non-combusting, prototype device is shown in Fig. 2. The operating cycle begins with the opening of the poppet valve, permitting compressed air to flow from the high-pressure reservoir to the driver side of the piston. The compressed air accelerates the piston into the reactant gases in the main cylinder. The flow area of the poppet, the pressure in the air reservoir, the piston mass, and the piston friction dictate the compression ratio. Diesel-style fuel injectors are used to dynamically inject fuel (and possibly other species) into the compressed gases, combustion occurs, and the free piston is driven back towards its original position via product expansion.

The method of implementing injection, mixing, and combustion is a critical aspect of this research since it affects the ability to achieve high combustion efficiency and low heat transfer as well as combustion phasing. We note that the pressures and temperatures for combustion at extreme states are significantly higher than in current engines. As an example, stoichiometric propane and air modeled as a well mixed ideal gas achieve a pressure of nearly 1200 bar and temperature of 3300 K when reacted adiabatically at a compression ratio of 100:1.

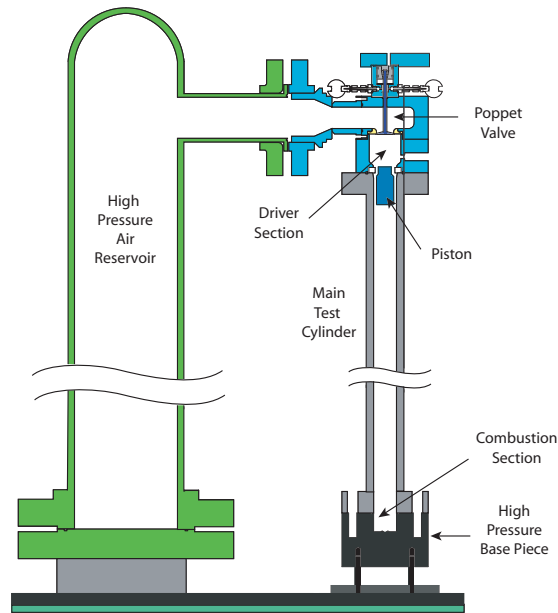


Figure 2: Cross-sectional view of the main test cylinder, valve assembly, and air reservoir.

Due to the high pressures involved in this strategy, our original intent was to implement a two-piston approach to achieving the extreme compression state since this would inherently balance the forces resulting from combustion and avoid the need to absorb a large reaction impulse. While we still believe that two pistons will be required in a practical engine, we have elected to simplify our prototype by using a single piston fired vertically downward. By operating vertically, we can easily supply the necessary reaction force (via the concrete floor), and reduce the infrastructure required for the demonstration device.

The free-piston architecture was chosen for its ability to attain high piston speeds and a long stroke. High piston speed reduces the time spent at high temperatures and therefore decreases heat loss. As designed, the prototype is capable of achieving mean piston speeds of ~ 80 m/s, almost an order of magnitude higher than current piston engines (but still a modest Mach number). Similarly, a large clearance height (the result of a longer stroke) reduces heat loss by reducing the surface-to-volume ratio.

Using a free piston adds complexity, however, in terms of position sensing. In order to track piston position we use a series of variable reluctance sensors mounted in holes that pass only partially through the non-ferritic, stainless-steel wall. By sensing position through the cylinder wall, we maintain bore integrity for high pressure and provide an uninterrupted wall surface for the piston rings. The sensors operate by producing a change in current proportional to the change in their magnetic field. By mounting a steel ring on the piston, we can detect when the piston has passed a particular sensor. By mounting two rings, we can determine an average velocity for the piston as it passes a particular sensor. By mounting 12 of these sensors along the length of the cylinder, we

will be able to construct the piston position profile for the non-combusting experiments. When combustion is implemented, the piston forces are more difficult to model, and a second sensing element (such as a Hall-effect sensor) located near minimum volume may be necessary to obtain the required resolution.

Hardware and System Progress

The composite experimental system consists of several subsystems each of which is currently undergoing an intensive, parallel development effort. The status of each subsystem is summarized below.

Test Cylinder and Air Reservoir: The main test cylinder and air reservoir have been fabricated, pressure tested, and delivered. The 2.5 m long test cylinder was honed to a 54.1 mm cylinder bore. This length yields approximately a unit aspect ratio at TDC for a compression ratio of 50:1 and a 2:1 bore to clearance height ratio for a compression ratio of 100:1. A separate base section that bolts on to the end of the cylinder and was honed integral with the cylinder, was designed for added strength and increased flexibility. While the main cylinder is constructed of a non-ferritic, austenitic stainless steel (304L), the base section is made of high-strength ferritic stainless (17-4PH). The non-ferritic stainless steel allows for sensing piston position through the wall of the cylinder without creating holes in the cylinder wall. The current base section was designed for operation without combustion and can withstand pressures in excess of 700 bar. The main test cylinder is rated to 415 bar. Because of the rapid pressure drop as the product gases expand, the main test cylinder does not need to be stronger, even for the combustion experiments. Only the base section is exposed to the extreme pressures. A second base section is currently being designed for the higher pressures due to combustion. This new section will again be honed to match the cylinder and will have provisions for both fuel injectors and sapphire windows for imaging. The air reservoir was designed to maintain 95% of its original pressure during the experiment. It is a 0.15 m³ tank rated for operation to 75 bar. The design includes flanges for valve connections and sensors as well as a large port for connecting to the poppet valve assembly.

Poppet Valve Assembly: The poppet valve mechanism was designed to provide a large flow area and a fast opening time. A cross-sectional view of the mechanism is shown in Fig. 3. High-pressure air from the reservoir pushes on the back on the poppet valve in the closed position. Helium, in a chamber near the top of the valve stem, holds the poppet valve closed by applying a force in opposition to that of the high-pressure air. To open the valve, the helium chamber is vented to the atmosphere through three fast solenoid valves. As the helium pressure below the valve piston drops, the high-pressure air forces the valve open. Concurrently, helium is permitted to flow into a chamber above the valve piston in order to hold the valve open for the remainder of the experiment.

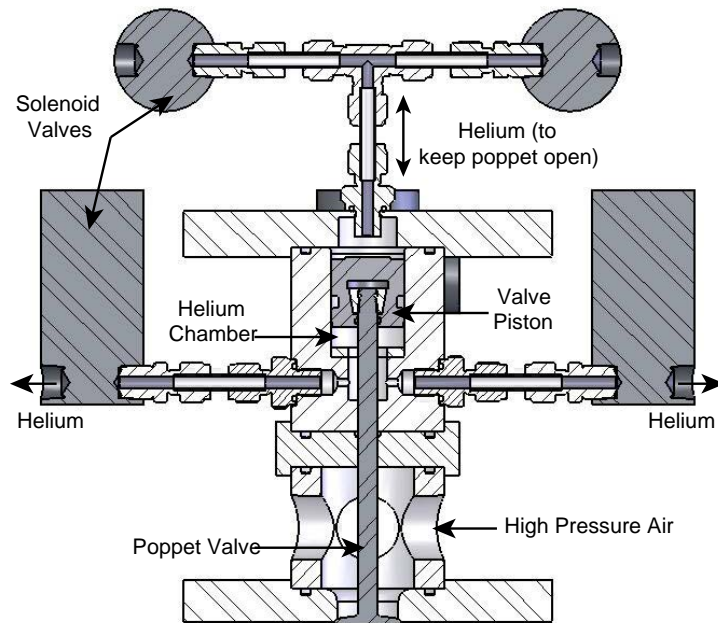


Figure 3: Prototype poppet valve cross-section. Solenoid valves vent the helium in the helium chamber which allows the high pressure air to open the poppet valve. Meanwhile, helium flows in above the valve piston to keep the poppet valve open throughout the experiment.

A prototype poppet valve was designed and built to test response time, flow rate, and repeatability. A small air reservoir and an LVDT were attached to the end of the poppet valve to permit monitoring of the opening profile. The opening profile from the LVDT, and the measured pressure drop in the air reservoir, can be used to determine the discharge coefficient of the poppet valve assembly. A discharge coefficient is used in the mass flow rate equations to account for flow losses and other unmodeled dynamics.

Examples of a measured opening profile and corresponding pressures are shown in Fig. 4 for a 25 mm-diameter valve. The black line in part (a) shows that the valve opening time is about 12 ms. The red line in part (b) shows the measured reservoir pressure while the black, dashed line shows the results of a simulation using a flow coefficient of 0.6. Since the valve opens into a tube which is in turn open to the environment but provides some flow impedance, the pressure downstream of the valve initially increases (since the valve opens so quickly) but then quickly drops back to ambient pressure. The measured pressure at this downstream location is shown in green on the figure.

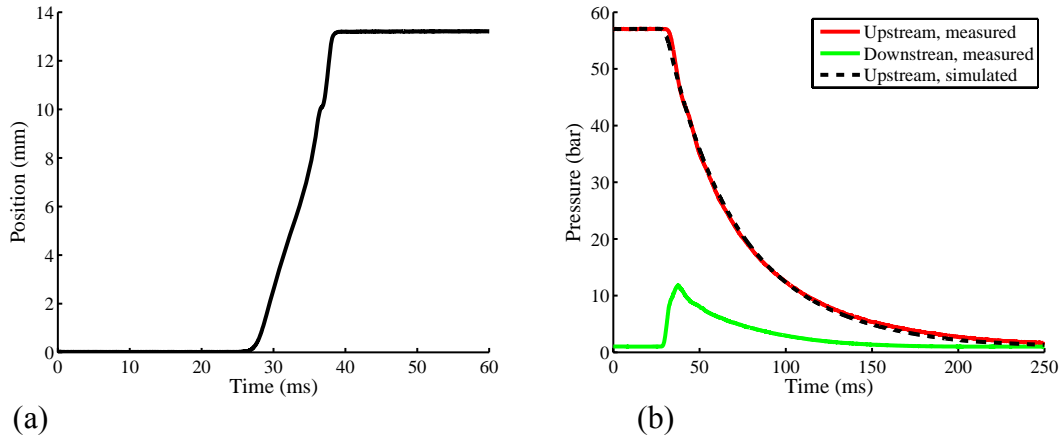


Figure 4: (a) The valve position as it opens. The opening time is 12.5 ms for a lift of 13.2 mm. (b) The measured air reservoir pressure upstream and downstream of the poppet valve along with the simulated reservoir pressure assuming a discharge coefficient of 0.6.

With the valve discharge coefficient and opening time determined experimentally, the required valve diameter can be established for any given range of compression ratio, piston mass, etc. For example, using the measured flow coefficient of 0.6 and our nominal piston mass and friction specifications, a valve diameter of 35 mm should be sufficient to achieve compression ratios in excess of 100:1.

Finally, the poppet valve prototype was also used to test repeatability—a critical issue when considering the possibility to construct a two-piston device. Tests were run with the same initial helium and air pressures to look at variability in the valve opening profile, specifically variability in the opening time. For the same initial pressures, the majority of opening times varied by less than 0.5 ms (out of ~12 ms). Our modeling results show that changes in valve opening time of 1 ms change the CR of our single-piston system by less than 1%. Figure 5 shows the piston dynamics (without combustion) for two linear valve opening profiles differing in opening time by 1 ms.

The valve discharge coefficient and repeatability are both within the ranges required to achieve the desired compression ratios. The next step is to finish the fabrication of the second version of the valve assembly with the larger poppet head diameter that will interface with the air reservoir and the main test cylinder.

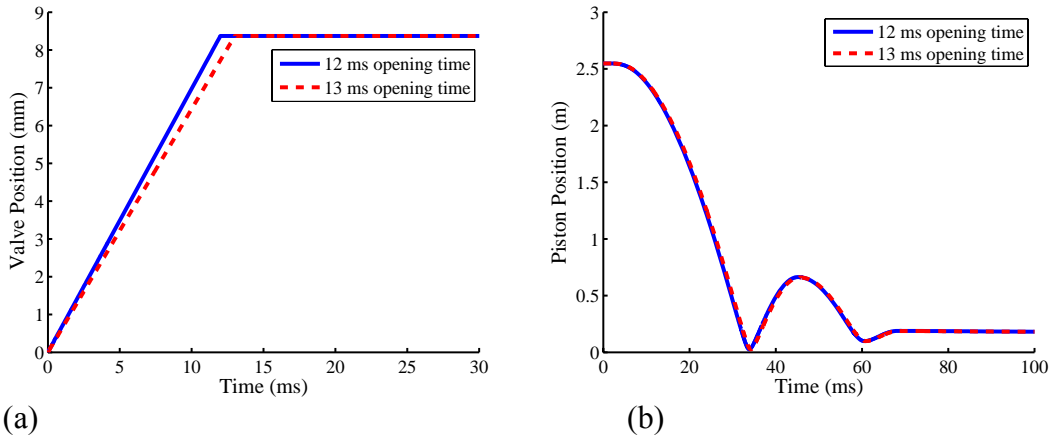


Figure 5: (a) Two linear opening profiles for a 35 mm valve where the max area occurs when the lift is 8.5 mm. (b) Piston trajectories for the two profiles in part a. The compression ratio varies by less than 1% for a 1 ms variation in opening time (99.9 vs 99.1). The variation is a function of the absolute change in opening time rather than a percentage change—an opening time change from 20 to 21 ms similarly produces a compression ratio variation less than 1%.

Data Acquisition System: The entire compression/expansion experiment lasts less than 100 ms but has many sensors that must be monitored simultaneously at high speed. For this purpose we have developed a data acquisition system built around the Iotech Daqboard 3000. This board has 16 single-ended analog inputs multiplexed at high speed through a single 16-bit A/D converter with a sample rate of 1 MHz. Even with all channels in operation, this system has sufficient bandwidth to accommodate both the variable reluctance sensors and static pressure sensors. For the dynamic pressure sensors observing the combustion event, a Gagescope data acquisition board has been obtained which has 12-bit resolution and two dedicated A/D channels, each at 10 MHz. Both boards are hosted by a PC and controlled using custom C++ code.

Ring Design: The high speeds and pressures necessary to accomplish combustion at extreme states place demands on piston ring design far beyond what is possible with existing piston rings. The combination of length of piston travel (~2 m) and high velocity (> 120 m/s peak) make it extremely difficult to maintain a proper oil film for hydrodynamic lubrication of the rings as is used in a conventional engine. Hence we have focused on developing ring designs that do not require an oil film and using materials with low sliding friction such as high-performance plastics and various graphite-filled composites.

Figure 6 illustrates the challenges involved, showing that the friction-induced heat transfer to the ring is so large at the speeds and pressures involved, that a conventional ring design would likely melt, even if we stepped down the energizing pressure to a small fraction ($1/10^{\text{th}}$) of the chamber pressure.

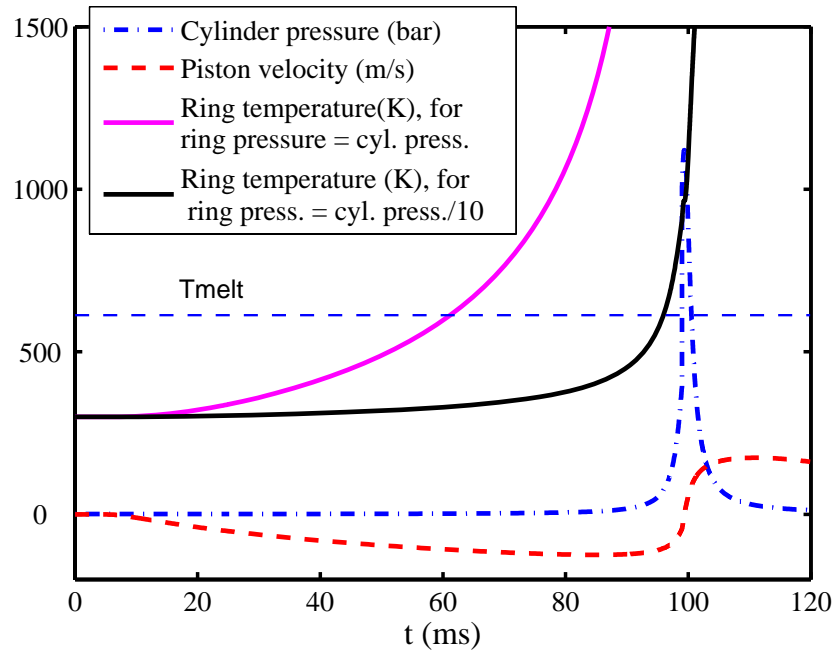


Figure 6: Maximum piston ring temperature for a simulated combustion cycle for rings energized with the same pressure as the combustion chamber and energized with $1/10^{\text{th}}$ the chamber pressure. The horizontal line shows the melting temperature of the ring. Ring properties are for carbon-impregnated PEEK. The maximum temperature occurs at the interface with the wall.

Fortunately, our modeling efforts show that at the speeds involved, use of a conventional, pressurized ring approach is not necessary. As Fig. 7 shows, a ringless design using a radial clearance of about 0.2 thousandths of an inch (~ 0.5 thousandths diametrically) would result in a total blowby of about 1%, well within acceptable limits. Experimental checks on a test apparatus at low pressures agreed very well with the model, lending credibility to the result. This result, combined with the results above for the energized ring, and the fact that our cylinder bore is honed to within a tolerance of 1 thousandth of an inch diametrically, has led us to move in the direction of a non-energized ring. Several designs have been considered to date. The most promising of these will be fabricated as test articles and evaluated under non-combusting conditions in the prototype apparatus to provide design data for the rings to be used under combusting conditions.

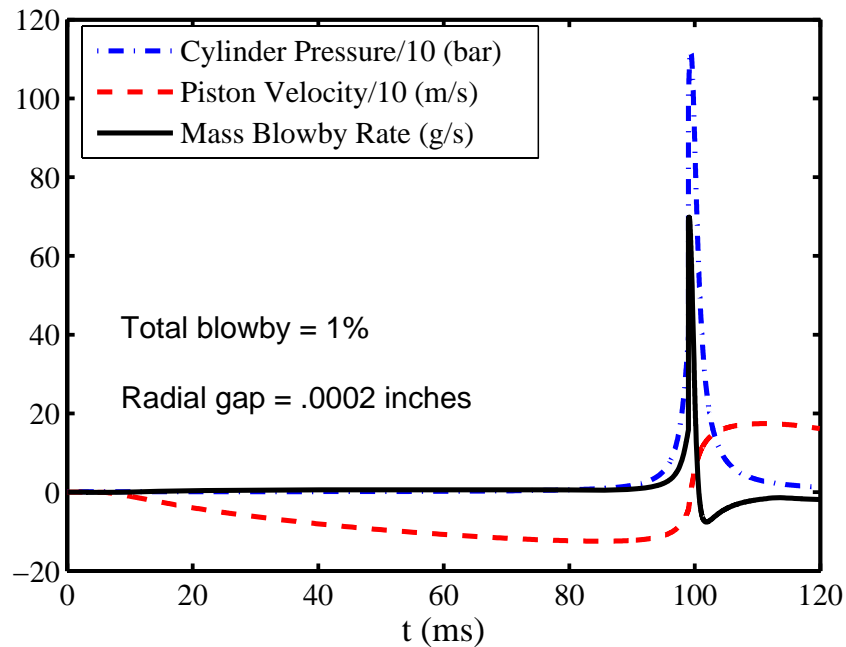


Figure 7: Gas mass flow rate past the piston for a simulated combustion cycle. The combustion chamber pressure and piston velocity shown on the plot are inputs to the flow model from the combustion cycle simulation. Flow is modeled as compressible flow through a small annulus with friction.

Mass Measurement System: One of our primary goals for the non-combusting experiments is to test ring designs. In order to do this we must have a method for measuring the blowby that occurs during an experiment. After evaluating a variety of ideas, we settled on a system that will directly measure the mass of gas contained in the cylinder before and after a run. The basic design consists of a light-weight aluminum tank placed on a high-precision scale. Prior to running, the entire system (cylinder + tank) is evacuated; the tank is filled with gas and then weighed. This gas is then used to fill the cylinder. The tank is evacuated and weighed again, and after the run the gas remaining in the cylinder is expelled to the tank and then weighed again. The mass remaining in other volumes such as the cylinder base, connecting tubes, etc. can be estimated with P,V,T measurements, however these masses are a small fraction of the mass directly weighed in the tank. As designed, the system should be able to tell us overall blowby within about 1% of the mass of the initial charge. (Values of blowby below this mark (1%) are considered negligible for our purposes.)

Task 2: Minimum Entropy Generation in a Generalized Reactive Engine

We have shown previously that irreversibility due to combustion can only be minimized when chemical reactions occur at very high internal energy (or enthalpy); see GCEP Technical Report [1]. The effort over the past year was focused on extending the analytical results beyond the ideal case (an adiabatic, homogeneous piston engine) to account for matter and heat transfers during engine operation. Here, we briefly describe the model, results, and implications for engines in which reactions occur in an *unrestrained* manner (*e.g.*, combustion) or in a *restrained* fashion (*e.g.*, electro-chemical reactions in fuel cell systems). The analysis and results are discussed in greater detail in Pub. 2.

The overall system being analyzed is a composite of the ideal gas mixture within the cylinder and the engine coolant, as shown schematically in Figure 8. However, the cooling system *CS* is assumed to have sufficient capacity that it operates at a quasi-steady state.* Thus, only the dynamics of internal energy U , entropy S , and chemical species $\mathbf{N} \in \mathcal{R}^n$ for the gas mixture within the cylinder need to be considered in the dynamical system formulation.

Finite-rate chemical kinetics, *i.e.*, where $f_j(U, V, \mathbf{N})$ is the net production rate of species j , are included in the model. The in-cylinder chemical composition can also be changed via active transfers (injection or removal) of chemical species δN_j^{in} , as well as passive transfers δN_j^b (*e.g.*, ring blowby, denoted here by the superscript b).† Similarly, the model includes passive heat loss δQ_{loss} from the piston engine, plus an additional active component of working fluid heating or cooling δQ^{in} .

It is assumed that the active transfers δN_j^{in} and δQ^{in} can be directly manipulated in the same manner that the change in volume dV is a control input in previous analysis (as active transfer of energy in the form of expansion work, $\delta W^{out} = PdV$). These transfers are to be contrasted with changes taking place entirely within the system boundary (*e.g.*, due to combustion) or *passive* transfers across the system boundary (*e.g.*, heat transfer to the engine coolant δQ_{loss} , or species transfer due to ring blowby δN_j^b) that are not amenable to precise control.

* The cooling system rejects energy transferred in as heat δQ_{loss} from the cylinder out to the surroundings, along with the associated entropy outflow $\delta Q_{loss}/T_0$.

† Blowby leads to species transfer δN_j^b out to the surroundings, and reacted to (as well as mixed with) the environmental species. Therefore, we will assume the molar enthalpy and entropy of the blowby species j are equal to the dead-state enthalpy $h_{j,0}$ and entropy $s_{j,0}$, respectively. In other words, all the exergy associated with the blowby species is destroyed.

The extent variable ξ measures reaction progress via the entropy difference between the actual system and its constant- UV counterpart:

$$\xi = 1 - \frac{S_{eq}(U, V, \mathbf{N}_{eq}) - S(U, V, \mathbf{N})}{L_{S,i}}$$

where $L_{S,i} = S_{eq}(U_i, V_i, \mathbf{N}_{eq,i}) - S(U_i, V_i, \mathbf{N}_i)$.

The optimization problem is solved using the Pontryagin maximum principle, which yields the Hamiltonian

$$H = c_V q_V + c_Q q_Q + \sum_j c_j q_j + (1 + \alpha) \sum_j \frac{\mu_j}{T} f_j - c_{loss} q_{loss} - \sum_j c_j^b q_j^b$$

where the coefficients for the active control variables are given by

$$c_V = -\alpha \left(\frac{P - P_{eq}}{T_{eq}} \right)$$

$$c_Q = -\alpha \left(\frac{1}{T} - \frac{1}{T_{eq}} \right) + \frac{1}{T^{in}} - \frac{1}{T}$$

$$c_j = -\alpha \left(\frac{h_j^{in} - T s_j^{in} - \mu_j}{T} - \frac{h_j^{in} - T_{eq} s_j^{in} - \mu_{j,eq}}{T_{eq}} \right) - \frac{h_j^{in} - T s_j^{in} - \mu_j}{T}$$

whereas the coefficients corresponding to the passive transfer rates q_{loss} and q_j^b are, respectively,

$$c_{loss} = -\alpha \left(\frac{1}{T} - \frac{1}{T_{eq}} \right) + \frac{1}{T_0} - \frac{1}{T}$$

$$c_j^b = -\alpha \left(\frac{h_{j,0} - T s_{j,0} - \mu_j}{T} - \frac{h_{j,0} - T_{eq} s_{j,0} - \mu_{j,eq}}{T_{eq}} \right) - \frac{h_{j,0} - T s_{j,0} - \mu_j}{T}$$

where α is a non-positive multiplier which enforces the complete-combustion requirement, *i.e.*, $\alpha \leq 0$.

By the maximum principle, the set of control inputs that minimizes the total entropy generated from the composite system (generalized piston engine plus cooling system) must also maximize the Hamiltonian above, *i.e.*,

$$(q_V^*, q_Q^*, \mathbf{q}^*) = \arg \max_{\Omega} H$$

over the admissible set

$$\Omega = \left\{ (q_V, q_Q, \mathbf{q}) \in R^{n+2} : |q_V| \leq q_{V,max}, |q_Q| \leq q_{Q,max}, |q_j| \leq q_{j,max} \right\}$$

We note that in the absence of heat and matter transfers, the preceding analysis reverts to exactly that presented in previous GCEP report for the ideal (adiabatic, homogeneous) piston engine (Pub. 1) [1]. Now, consider instead the more general model that incorporates heat and species transfers. At the limit of $T^{in} = T$ and $h_j^{in} - T s_j^{in} = \mu_j$ for a homogeneous system, the optimal control synthesized above simplifies substantially. The coefficients for the active control variables now take on similar functional forms:[§]

$$c_V = -\alpha \left(\frac{P - P_{eq}}{T_{eq}} \right), \quad c_Q = -\alpha \left(\frac{1}{T} - \frac{1}{T_{eq}} \right), \quad \text{and} \quad c_j = \alpha \left(\frac{h_j^{in} - T_{eq} s_j^{in} - \mu_{j,eq}}{T_{eq}} \right)$$

Assuming that the instantaneous rates of heat rejection q_{loss} and chemical kinetics f_j are independent of these control variables, maximizing Hamiltonian H in accordance with the maximum principle then translates into extremal (bang-bang) controls

$$q_V^* = \begin{cases} -q_{V,max} & \text{(compression) if } P < P_{eq} \\ +q_{V,max} & \text{(expansion) if } P > P_{eq} \end{cases}$$

$$q_Q^* = \begin{cases} -q_{Q,max} & \text{(cooling) if } T > T_{eq} \\ +q_{Q,max} & \text{(heating) if } T < T_{eq} \end{cases}$$

$$q_j^* = \begin{cases} -q_{j,max} & \text{(species removal) if } h_j^{in} - T_{eq} s_j^{in} > \mu_{j,eq} \\ +q_{j,max} & \text{(species injection) if } h_j^{in} - T_{eq} s_j^{in} < \mu_{j,eq} \end{cases}$$

From the thermodynamic standpoint, the Hamiltonian H can be decomposed into four components. Gibbs' equation for the actual system will take the form

$$\begin{aligned} TdS &= dU + PdV - \sum_j \mu_j dN_j \\ &= dU + PdV - \sum_j \mu_j (f_j dt + \delta N_j^{in} - \delta N_j^b) \end{aligned}$$

On the other hand, the equilibrium Gibbs' equation is

$$T_{eq} dS_{eq} = dU_{eq} + P_{eq} dV_{eq} - \sum_j \mu_{j,eq} (\delta N_j^{in} - \delta N_j^b)$$

By relating the two equations at fixed U , V , and atomic composition, we obtain

$$d(S_{eq} - S) = \left(\frac{1}{T_{eq}} - \frac{1}{T} \right) dU + \left(\frac{P_{eq}}{T_{eq}} - \frac{P}{T} \right) dV + \sum_j \frac{\mu_j}{T} f_j dt - \sum_j \left(\frac{\mu_{j,eq}}{T_{eq}} - \frac{\mu_j}{T} \right) (\delta N_j^{in} - \delta N_j^b)$$

or

[§] The coefficients for passive transfers c_{loss} (for heat loss) and c_j^b (for species blowby) remain unchanged.

$$\begin{aligned} \frac{d(S_{eq} - S)}{dt} = & \left(\frac{1}{T_{eq}} - \frac{1}{T}\right)(q_Q - q_{loss}) - \left(\frac{P - P_{eq}}{T_{eq}}\right)q_V + \sum_j \frac{\mu_j}{T} f_j \\ & + \sum_j \left(\frac{h_j^{in} - T_{eq}s_j^{in} - \mu_{j,eq}}{T_{eq}}\right)q_j - \sum_j \left(\frac{h_{j,0} - \mu_{j,eq}}{T_{eq}} - \frac{h_{j,0} - \mu_j}{T}\right)q_j^b \end{aligned}$$

Identifying terms in the equation above with those in the Hamiltonian H for the generalized system will reduce H to the form below (with $\alpha \leq 0$),

$$H = \alpha \frac{d}{dt}(S_{eq} - S) - \left(\frac{1}{T_0} - \frac{1}{T}\right)q_{loss} + \sum_j \frac{\mu_j}{T} f_j + \sum_j \left(\frac{h_{j,0} - Ts_{j,0} - \mu_j}{T}\right)q_j^b$$

involving the following terms:

1. The change in entropy difference between the actual system and its constant- UV counterpart, $d(S_{eq} - S)$;
2. Entropy generation due to engine cooling, $(\delta S_{gen})^{CS} = (T_0^{-1} - T^{-1})q_{loss}dt$;
3. Entropy generation due to chemical reactions, $(\delta S_{gen})^{chem} = -T^{-1}\sum_j \mu_j f_j dt$; and
4. Entropy generation due to ring blowby, $(\delta S_{gen})^b = -T^{-1}\sum_j (h_{j,0} - Ts_{j,0} - \mu_j) q_j^b dt$.

Recall that based on Pontryagin's maximum principle, maximizing Hamiltonian H is the necessary condition for minimizing entropy generation in the model engine. The equation above shows that the optimal strategy reduces to minimizing $S_{eq} - S$, *i.e.*, the entropy that *would be generated after time t* so as to approach chemical equilibrium and thus complete combustion. This is accomplished at every instant t via active controls of the various modes of energy transfers—gas expansion or compression $\pm q_{V,max}$, heating or cooling $\pm q_{Q,max}$, as well as species addition or removal $\pm q_{j,max}$.

It is not hard to conceptualize the case for transfers of certain chemical species *into* the system, *e.g.*, using fuel injectors or a variable valve actuation system.. On the other hand, *selective* species transfers *out of* the system and precise control of heat transfer remains technically challenging. By contrast, piston motion, and thus work transfer, can be implemented with precision, *e.g.*, actuated mechanically using a variety of methods (including a slider-crank mechanism).

We note that when heat and species transfers are included in the piston engine model, by convention, the temperature T^m at which heat transfer takes place, and the enthalpy h_j^{in} and entropy s_j^{in} of the species being transferred are specified. By contrast, the pressure P^{out} at the work transfer boundary (*i.e.*, at the face of the piston) is never stated; it is simply taken to be equal to the cylinder pressure P .

It is crucial to understand the thermodynamics behind this difference. Each mode of transfer across the system boundary at some transfer *rate* (sometimes normalized to unit area and expressed as a *flux*) will take place only if there exists a thermodynamic *driving*

force—temperature difference for heat, chemical potential difference for a chemical species, pressure difference for expansion work. The subsequent rate at which the system pressure equalizes is quite rapid, since pressure perturbations propagate at the speed of sound. By contrast, the rates at which the gas mixture within system boundary equilibrate thermally (with respect to heat transfer) and in terms of composition (with respect to species transfer) are relatively slow due to the nature of the transfer mechanism, which is via the advection and diffusion of matter within the system.

This discussion has relevance to the generalized piston engine analysis above as well as to the study of other engine systems. In all cases in which system homogeneity is assumed, it means that the fluxes and driving forces for heat and matter transfers must be small and occur at the diffusion length scale:**

1. The prerequisite of low fluxes sets the thermodynamic bounds $q_{Q,max}$, $q_{j,max}$, and $q_{V,max}$ for the control variables.
2. The condition of small driving forces implies that heat transfer has to take place close to the system temperature at all times, $T^{in} \approx T$. Similarly, the chemical potentials of species being transferred must be close to the species potentials within the system, $h_j^{in} - T^{in}s_j^{in} \approx \mu_j$. These approximations were made at the outset of the optimal control analysis above.
3. Lastly, the requirement of “distributed” transfers at the diffusion length scale eliminates spatial gradients in temperature and concentration which induce additional entropy generation.

These conditions are taken for granted in the case of expansion work transfer (since piston engines do not operate near the limit set by thermodynamics, namely, the speed of sound), but are far more difficult to realize in the case of heat and matter transfers.

The engine model analyzed above involves combustion, *i.e.*, rapid conversion of chemically-frozen reactants to equilibrium products with the attendant conversion of energy stored in chemical bonds to sensible energy. This approach to chemical conversion is characterized by significant entropy generation $(S_{gen})^{chem} = \int -T^{-1} \sum \mu_j f_j dt$. We note that the integrand $-T^{-1} \sum \mu_j f_j \geq 0$ is a function of the state variables U , V , and \mathbf{N} only, not of the controls q_V , q_Q , and \mathbf{q} . In this sense, combustion reactions are *unrestrained*.

Other chemical reactions (e.g., the electrode reactions in a fuel cell) can be carried out in a *restrained* manner, which corresponds to the limit that the quantity $-T^{-1} \sum \mu_j f_j$ equals zero—in other words, that the reacting system starts off at equilibrium—and the requirement that it remains so via control. These two conditions imply that the total entropy generated $(S_{gen})^{chem}$ due to reactants-to-product conversion, at the limit, also equals zero—which accounts for the appeal of such systems from the efficiency standpoint.

** To pinpoint molecular diffusion as the transfer mechanism also requires that the driving forces be small so as not to induce advection, *i.e.*, bulk gas motion within the system boundary.

We observe that the decrease in entropy generation presupposes that the restrained reaction is effected by active transfer of work, heat, or chemical species which is itself accomplished efficiently, with minimal generation of entropy. This will be true for energy transfer with gas expansion or compression, and less so for heat or species transfers, as noted in the discussion earlier. For instance, the overpotential (driving force) needed for electron transfers (species flux) to take place in a fuel cell electrode, thereby driving the electrode reaction forward, is a significant source of inefficiency.

Future Plans

We are currently setting up the cylinder, reservoir, poppet valve, and safety systems so that we can begin to non-combusting experiments. The first tests will include candidate ring designs to evaluate ring wear and sealing performance as mentioned previously. We will also evaluate the repeatability of achieving a specific compression ratio. Once the ring friction has been well modeled and the repeatability of achieving a desired compression ratio has been established, we can begin combustion experiments. It is our hope to achieve our first combustion experiments by the end of this summer (September 2007).

Work on the theoretical aspects of engine efficiency will focus on completing our evaluation of steady-flow (gas turbine) combustion engines with a view towards proposing a set of concrete measures to be subsequently demonstrated experimentally. The work will then be formally extended to include regenerative engine architectures as a next step towards building a comprehensive-but-systematic approach to achieving ultra-high engine efficiency.

Publications

1. Teh, K.-Y., and Edwards, C. F. An Optimal Control Approach to Minimizing Entropy Generation in an Adiabatic Internal Combustion Engine. Submitted to *J. Dynamic Systems, Measurement and Control*.
2. Teh, K.-Y. Thermodynamics of Efficient, Simple-Cycle Combustion Engines. Ph.D. dissertation, Dept. of Mech. Eng., Stanford Univ., Stanford, CA, 2007.

References

1. Edwards, C. F., Caton, P. A., Miller, S. L., Svrcek, M. N., and Teh, K.-Y., Development of Low-Irreversibility Engines. GCEP Tech. Rep., 2006.
2. Van Blarigan, P., S Goldsborough, N. Paradiso, J. Wu, Homogeneous Charge Compression Ignition Free Piston Linear Alternator: Sandia National Labs, SAND99-8206, November, 1998.

Contacts

Christopher F. Edwards: cfe@stanford.edu